ChemComm

Accepted Manuscript

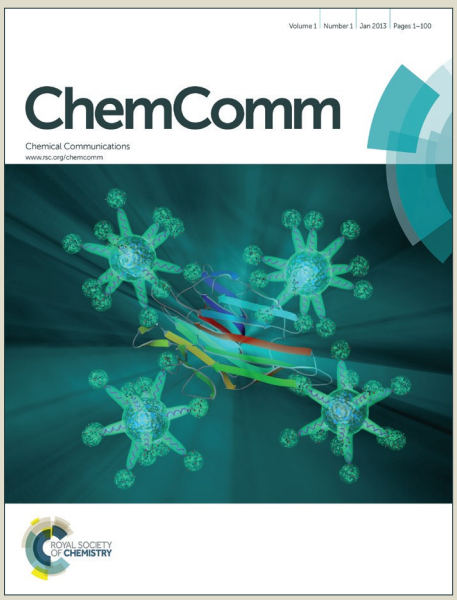

This is an *Accepted Manuscript*, which has been through the Royal Society of Chemistry peer review process and has been accepted for publication.

Accepted Manuscripts are published online shortly after acceptance, before technical editing, formatting and proof reading. Using this free service, authors can make their results available to the community, in citable form, before we publish the edited article. We will replace this *Accepted Manuscript* with the edited and formatted *Advance Article* as soon as it is available.

You can find more information about *Accepted Manuscripts* in the Information for Authors.

Please note that technical editing may introduce minor changes to the text and/or graphics, which may alter content. The journal's standard Terms & Conditions and the Ethical guidelines still apply. In no event shall the Royal Society of Chemistry be held responsible for any errors or omissions in this *Accepted Manuscript* or any consequences arising from the use of any information it contains.

ROYAL SOCIETY OF CHEMISTRY

www.rsc.org/chemcomm

Please do not adjust margins

Journal Name

COMMUNICATION

In situ monitoring of catalytic process variations in a single nanowire by dark-field-assisted surface-enhanced Raman spectroscopy†

Received 00th January 20xx,
Accepted 00th January 20xx

DOI: 10.1039/x0xx00000x

www.rsc.org/

Xin Shi[a], Haowen Li[a], Yi-Lun Ying[a], Chang Liu[b], Li Zhang[b], Yi-Tao Long*[a]

In this communication, we provide a new method for characterizing the kinetics of a catalytic process on multiple sites of a single nanowire by dark-field-assisted surface-enhanced Raman spectroscopy (DFSERS). The differences in reaction rate and the extent of the photocatalysis between sites of a single nanowire were observed.

Real-time in situ monitoring of catalytic processes at the nanoscale would provide direct and detailed information on the catalyst performance[1]. Among the various nanostructures, one-dimensional (1D) nanostructures have already drawn increasing attention due to their catalytic activity, thermal stability and electrical conductivity[2]. These properties stimulated their applications in areas such as sensing[3], pollution treatment, charge storage and energy conversion[4]. Revealing the molecular distribution, conversion and the catalytic process on a single nanowire would be of considerable benefit for designing various types of nanowire-based materials with improved catalytic performance, prolonged lifetime and clearer mechanism[5].

Surface-enhanced Raman spectroscopy (SERS) has emerged as a powerful new frontier in the study of chemistry, physics, materials science and bioscience[6]. Recently, SERS has been considered a potential method for online monitoring of catalytic processes[7]. By using several excellent bifunctional materials that exhibit both catalytic and SERS activity, both the reaction kinetics and the variation in not only the catalyst itself but also the molecules adsorbed on the catalyst could be studied under working conditions[8]. Although the dynamic process of a single active site could be studied by SERS, such point measurements would only reflect information on a "bulk" scale, and provide limited spatial-resolved information.

Herein, we demonstrate a novel method for parallel monitoring of the catalytic process of the entire and multiple sites of a single nanowire by dark-field-assisted surface-enhanced Raman spectroscopy (DFSERS) (Fig. 1). Comparing to previously reported literatures, our approach is novel in allowing parallel monitoring and characterizing of reaction kinetics on multiple sites of a single nanowire as well as revealing differences in the reaction process, such as the generation of different intermediates, at these sites. Besides, our method makes a single nanowire a nanoreactor for multiplexing reaction analysis, i.e. performing different reactions on different sites along a single nanowire, making it possible to compare and study in the same working conditions. Here, the reduction of p-nitrothiophenol (pNTP) to p-aminothiophenol (pATP) with sodium borohydride occurring on a MnOOH-Ag nanodisk composite nanowire catalyst was used as a model reaction. The Ag Nano disks on nanowire composite material plays a dual role in the process, as a catalyst of the reduction and a SERS-active analysis platform, while the MnOOH nanowire play an active part in the catalysis and yield a synergistic effect, which leads to their better catalytic performance.

A scanning electron micrograph and the dark-field image of a single hybrid nanowire are shown in Fig. 1c and Fig. S1. Nanowire catalysts with a length of approximately 10 μm were used for the following experiments. The nanowire catalysts were immobilized on a quartz glass. Then the surface of the nanowire catalysts was functionalized with 2-naphthalenethiol (2-NT) as an internal standard for relative quantification in SERS measurements, as demonstrated by pioneer work[8c]. By the use of a lab-built Raman spectroscopy system with dark-field illumination, SERS spectra from multiple sites of a single nanowire and their variation could be obtained.

[a] Key Laboratory for Advanced Materials and Department of Chemistry, East China University of Science and Technology, Shanghai, 200237 (P. R. China)
E-mail: ytlong@ecust.edu.cn.
[b] College of chemistry and materials science, Anhui Normal University, Wuhu 241000, P. R. China
Shanghai, 200237 (P. R. China)
* E-mail: ytlong@ecust.edu.cn

Electronic Supplementary Information (ESI) available: Supplementary table and figures. See DOI: 10.1039/x0xx00000x

ChemComm Accepted Manuscript

Please do not adjust margins

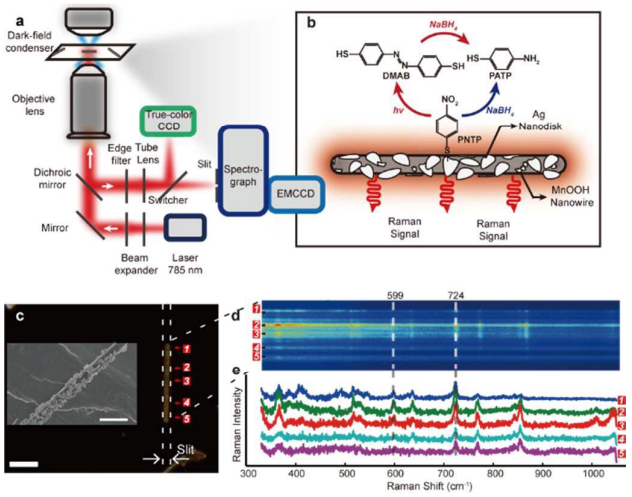

Fig. 1 Schematic of experimental set-up and spatial-resolved SERS spectral image. (a) Schematic of experimental set-up. DFC: dark-field condenser, DM: dichroic mirror, BE: beam expender, M: mirror. (b) Schematic of the MnOOH nanowire and the model reactions. (c) Dark-field image of a single MnOOH-Ag nanowire (scale bar: 6 μm). Inset: scanning electron micrograph of a MnOOH-Ag nanowire, scale bar: 1.5 μm. (d) SERS spectral image of the pNTP and 2-NT coated nanowire corresponding to the dark-field image in (c). (e) Five SERS spectra obtained from corresponding positions in the spectral image in (d)

Differ from the previously reported work on DF-SERS and nanowire SERS[9], in our approach, the dark-field microscopy was used for rapid locating and adjusting the position of nanowire of interest, and making the position of single nanowire fit for the entrance slit of the spectrometer. In that case, SERS signal from each part of the single nanowire could be excited. Therefore, all the scattered photons including the Rayleigh scattering and SER scattering could enter the spectrometer and be analysed. Then a spectral image containing spatial resolved SERS spectra could be obtained. The optical path is presented in Fig. 1a. The details of the experiment facilities and measurement procedures are shown in ESI.

With this method, Raman spectra containing both temporal and spatial information can be acquired along the nanowire material, so that the spectra variations along the whole nanowire or at any site of it could be studied individually. Although the spatial resolution is limited by the diffraction limitation of about 300-500 nm, the spatial resolved information could be obtained with high speed easily by virtue of such scanning-free method. Fig. 2 shows the first-order spectral image of a nanowire covered by pNTP (reactants) and 2-NT (internal standard). In the spectral image, the Y axis contains the spatial information along the one-dimensional structure, and the X axis indicates the Raman shift. By comparing the dark-field image and the SERS spectral image, the specific correspondence of the positions could be established. The different Raman enhancement effect at each site of the nanowire could be displayed in the spectral image. The intensity gradient along the single wire might be attributed to the inhomogeneity of the Ag nanodisks' geometry and distribution on the wire. The SERS spectra of pNTP, 2-NT, and pATP on single hybrid catalyst wires are displayed in Fig. S2.

The hydride reaction of 4-nitrophenol (4-NP) catalysed by metal nanoparticles has become one of the most used benchmarks for evaluating the catalytic activity of metal particle-based catalysts [10,11].The reduction of pNTP, an analogue of 4-NP, is usually been used as a drosophila reaction for SERS and TERS studies. To investigate the kinetics of the reaction by SERS, pNTP and 2-NT was pre-adsorbed on the catalysts and their characteristic bands were used for tracking the reaction process. A series of first-order spectral images of the nanowire, with 700 ms exposure time and approximately 300 ms for reading out, could be collected, which indicate the compound variation on the nanowire in the reduction. SERS spectra of the entire nanowire could be obtained by summing up the intensities of each pixel column of the first-order spectral image. The SERS spectrum changes of an entire single wire are shown in Fig. 2a with a range of Raman shift between ~350 cm^{-1} and ~1000 cm^{-1}. An instance displaying the spectrum changes with a Raman shift between ~300 cm^{-1} and ~1800 cm^{-1} is shown in Fig. S3, with a lower spectral resolution.

The spectra exhibit characteristic bands of pNTP and 2-NT before the reduction, and no special changes could be observed in the range of 300-1000 cm^{-1}. After the addition of sodium borohydride, the characteristic band of pNTP at 724 cm^{-1} assigned to C-S stretching vibrations decreased gradually, and a pATP band at 392 cm^{-1} appeared, relative to the typical 2-NT ring deformation band at 599 cm^{-1}, indicating the consumption of the reactants and formation of the products.

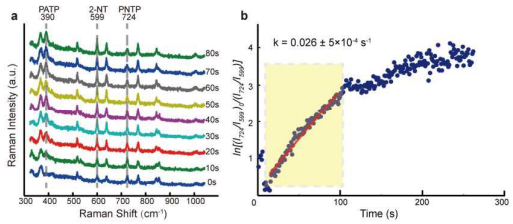

Fig. 2 Monitoring the catalytic reaction on an entire single nanowire with SERS. (a) Selected spectra of the same process, taken every 10 s after the addition of sodium borohydride. (b) Plot of $\ln[(I_{724}/I_{599})_0/(I_{724}/I_{599})]$ versus time for the determination of the rate constants for the reduction process with spectra shown in a. Data between 16-100 s after the addition of the sodium borohydride is fitted linearly.

To investigate the feasibility of this method for characterising the kinetics of single nanowire catalysis of a reduction process, the intensity of the pNTP band at 724 cm^{-1} was quantified relative to the intensity of the 599 cm^{-1} band of 2-NT. The logarithm of the ratio of the relative intensities after the addition of the borohydride was plotted in Fig. 2b. The intensity data was collected from the spectra at approximately 1 frame/s, and a total of 250 spectra were analysed here. The high concentration of sodium borohydride used in the experiment could be assumed as a constant during the initial reduction, and the reaction followed pseudo-first-order kinetics. The reaction rate constant could be determined by the equation (a)[8c]:

ChemComm Accepted Manuscript

This journal is © The Royal Society of Chemistry 20xx

$$k \cdot t = \left(\frac{[pNTP]_{t=0}}{[pNTP]_t}\right) = \ln\left(\frac{\left(\frac{I_{724}}{I_{599}}\right)_{t=0}}{\left(\frac{I_{724}}{I_{599}}\right)}\right) \quad \text{(a)}$$

Here, [pNTP] is the concentration of pNTP, and I_{724} and I_{599} are the intensities of the bands at 724 cm^{-1} and 599 cm^{-1}, respectively.

All the time-resolved SERS spectra and the bands intensity variations were collected from a single nanowire, hence the new, average-free insight provided by the optical isolation of a single nanomaterial could be introduced for more detailed information of the chemical process at the nanoscale. In this way, dissimilarities between single nanowires and between different active sites of a same wire could be revealed.

Due to the heterogeneity of the composite material, reaction performance might be different at different sites of the nanowire. In our approach, the SERS signal from multiple sites of the one-dimensional nanomaterial could be obtained and analysed individually. Fig. S4 shows a series of selected spectral images with a wavelength range of 300-1000 cm^{-1} from which reactions at each site of the nanowire could be analysed. Three SERS spectra of a certain nanowire were displayed (Fig. 3a), illustrating the differences at sites of the nanowire 80 s after adding the sodium borohydride. The intensity ratio I_{724}/I_{599} of site p3 is significantly lower than that at sites p2 and p1 after 80 s, which indicates the higher consumption of the reactant, pNTP. Furthermore, the reaction rates of the catalytic reaction could be characterised by the relative band intensities discussed above. Fig. 3b shows the relative intensities of these different sites varying in the first 170 s, corresponding to p1, p2 and p3, which display the differences in reaction rate. Site p2 shares a similar rate constant with the data from the entire wire, and p3 and p1 exhibit higher and lower values, respectively. Because of the significantly higher intensity of the SERS response from site p2, the slight discrepancies of p1 and p3 might be ignored in a bulk experiment.

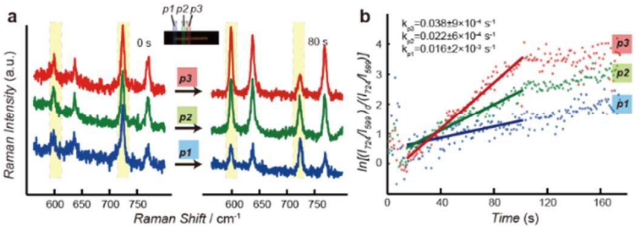

Fig. 3 Spatiotemporal variations of SERS spectra in the reaction. (a) SERS spectra of the three different sites discussed in the main text, p1, p2 and p3, before (0 s) and 80 s after the addition of sodium borohydride. Inset: corresponding dark-field micrograph of the same nanowire. Three sites were marked as 'p1', 'p2' and 'p3'. (b) Separate reaction rate analyses of the three sites, based on the intensity ratio of the band of pNTP at 724 cm^{-1} and of 2-NT at 599 cm^{-1} in the SERS spectra shown in (a).

Previous research has discussed the photocatalytic reaction in the pNTP reduction caused by the focused laser of the SERS monitoring[12] and one of its photocatalytic products, 4, 4'-dimercaptoazobenzene (4,4'-DMAB), would be produced through the SERS monitoring[12-13](Fig. 4). These two catalytic processes may occur on a single structure at the same time, which makes it difficult to distinguish these two approaches. Using our method, it would be easy to reveal the different reaction routes on a single wire. Fig. 4a shows a series of SERS spectra that varied with a Raman shift from ~1000 cm^{-1} to ~1600 cm^{-1}, collocated from an entire nanowire. The characteristic band of pNTP at 1331 cm^{-1} decreases significantly compared to the band at 1378 cm^{-1}, indicating the consumption of pNTP. As previous works reported[8a, 12-13, 13e], the generation of the photocatalytic product, DMAB, can be indicated by its characteristic bands at 1142 cm^{-1}, 1391 cm^{-1} and 1437 cm^{-1}. The SERS spectra of the entire single nanowire variation displayed a weak intensity at 1142 cm^{-1}, whereas the bands at 1391 cm^{-1} and 1437 cm^{-1} are much weaker, proving that the photocatalytic process is only a tiny fraction of the entire process under the experimental conditions. To reveal the different spatial distributions of the two catalytic processes, the spectral image from 6 s after adding sodium borohydride is displayed in Fig. 4b, from which the dissimilarities of the SERS spectra from different sites on the wire can easily be observed. Fig. 4c shows spectra from segments p4 and p5 in Fig. 4b, respectively. An obviously higher intensity of the DMAB bands at 1141 cm^{-1}, 1393 cm^{-1}, and 1438 cm^{-1} could be observed at p4, whereas the intensity of the 1331 cm^{-1} band at p4 is weaker. By analysing the space-dependent SERS spectra, it is revealed that there was more pNTP transformed into DMAB via photocatalytic process at site p4 than at p5. Fig. 4d and 4e display the time-resolved spectra variations of molecules on p4 and p5. After starting the reaction, at segment p4, a large part of pNTP converted into DMBA, which induced a significant high intensity at bands 1142 cm^{-1}, 1393 cm^{-1} and 1438 cm^{-1}. Then, DMAB was reduced into pATP by sodium borohydride. At the same period of time at site p5, these characteristic bands were almost invisible, and the intensity of the band at 1331 cm^{-1} decreased more gradually. Based on this method, the different catalytic routes can be studied while avoiding confusion from each other. The spectral images variations during the reaction on a single nanowire with a Raman shift between ~300 cm^{-1} and ~1800 cm^{-1} is displayed as a supplementary movie.

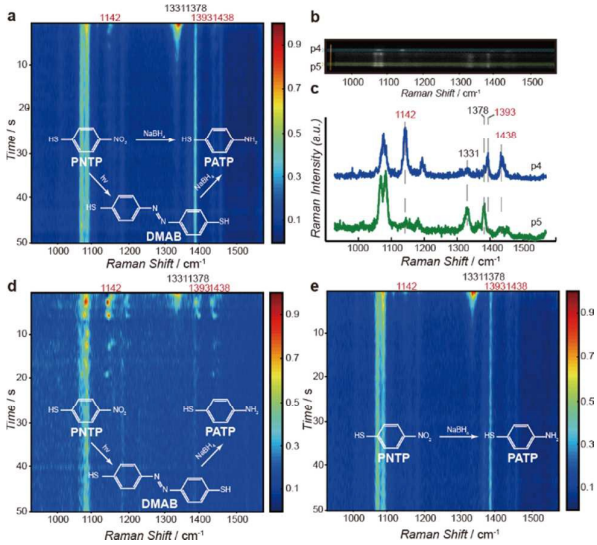

ChemComm Accepted Manuscript

Fig. 4 Spatial otherness of DMAB production via a photocatalytic process. (a) Colour-coded intensity map of time-dependent single-nanowire SERS measurements after the addition of sodium borohydride, with a range of Raman shift between 900 cm-1 to 1600 cm-1. (b) Spectral images of a single nanowire acquired at the 6th s after addition of the sodium borohydride. The corresponding dark-field micro-graph is shown on the left. The two segments analysed be-low are marked as 'p4' and 'p5'. (c) Raman spectra corresponding to segments p4 and p5. (d, e) Colour-coded intensity map of time-dependent SERS spectra of p4 and p5, respectively, at the same period of time as (a).

In this model reaction, we consider the following hypothec might be possible. The origin of such reaction performance variations might originate from the size, shape and distribution of Ag nanoparticles which influence the catalytic performance of the material. The nanoparticle-catalysed reaction may be more likely to occur on large and coupled Ag particles, while the small Ag particles might take part in the nanoparticle-catalyzed reaction[8e].

In conclusion, the present work demonstrates a novel dark-field-assisted SERS method for real time and *in situ* monitoring the reaction performance variation of multiple sites along a single nanowire. Most of previous literatures could obtain the mixed spectra of the two kind of reduction of pNTP, however this is, to our best knowledge, the first instance of monitoring the dissimilarities of a chemical process on different sites of a single nanowire in real time, under exactly same reaction conditions. Inhomogeneity of a solid nanocatalyst might be inevitable, hence such space- and time-resolved methods are vital for understanding the spatiotemporal gradients of catalytic performance. Our approach also make it possible to study the relationship between the SERS hot spots and the hot electron generation for its ability to reveal the variation of SERS enhancement and active sites of plamon-catalyzed reaction.

This research was supported by the National Natural Science Foundation of China (21327807, 21421004, and 21125522), Shanghai Pujiang Program (12JC1403500), and Program for Professor of Special Appointment (Eastern Scholar) at Shanghai Institutions of Higher Learning (YJ0130504).

Notes and references

1. B. M. Weckhuysen, *Angew. Chem. Int. Ed.* , 2009, **48**, 4910-4943.
2. (a) H. J. Choi, H. K. Seong, J. Chang, K. I. Lee, Y. J. Park, J. J. Kim, S. K. Lee, R. R. He, T. Kuykendall and P. D. Yang, *Advanced Materials*, 2005, **17**, 1351-1356; (b) C. K. King'ondu, A. Iyer, E. C. Njagi, N. Opembe, H. Genuino, H. Huang, R. A. Ristau and S. L. Suib, *J. Am. Chem. Soc.*, 2011, **133**, 4186-4189; (c) M. Pradhan, A. K. Sinha and T. Pal, *Chem. Eur. J.*, 2014, **20**, 9111-9119.
3. (a) Y. Cui, Q. Wei, H. Park and C. M. Lieber, *Science*, 2001, **293**, 1289-1292; (b) T. Kang, S. M. Yoo, M. Kang, H. Lee, H. Kim, S. Y. Lee and B. Kim, *Lab Chip*, 2012, **12**, 3077-3081.
4. (a) A. Debart, A. J. Paterson, J. Bao and P. G. Bruce, *Angew. Chem. Int. Ed.* , 2008, **47**, 4521-4524; (b) L. Mai, X. Tian, X. Xu, L. Chang and L. Xu, *Chem. Rev.*, 2014, **114**, 11828-11862.
5. D. A. Clayton, T. E. McPherson, S. Pan, M. Chen, D. A. Dixon and D. Hu, *Phys. Chem. Chem. Phys.*, 2013, **15**, 850-859.
6. (a) S. Schlucker, *Angew. Chem. Int. Ed.*, 2014, **53**, 4756-4795; (b) A. Indrasekara, S. Meyers, S. Shubeita, L. Feldman, T. Gustafsson and L. Fabris, *Nanoscale*, 2014, **6**, 8891-8899; (c) B. Peng, G. Li, D. Li, S. Dodson, Q. Zhang, J. Zhang, Y. H. Lee, H. V. Demir, X. Yi Ling and Q. Xiong, *ACS nano*, 2013, **7**, 5993-6000; (d) L. A. Lane, X. Qian and S. Nie, *Chem. Rev.*, 2015, **114**, 11828-11862; (e) T. Yang, X. Guo, H. Wang, S. Fu, J. Yu, Y. Wen and H. Yang, *Small*, 2014, **10**, 1325-1331.
7. (a) K. N. Heck, B. G. Janesko, G. E. Scuseria, N. J. Halas and M. S. Wong, *J. Am. Chem. Soc.*, 2008, **130**, 16592-16600; (b) K. F. Domke, T. A. Riemer, G. Rago, A. N. Parvulescu, P. C. Bruijnincx, A. Enejder, B. M. Weckhuysen and M. Bonn, *J. Am. Chem. Soc.*, 2012, **134**, 1124-1129; (c) H. Kim, K. M. Kosuda, R. P. Van Duyne and P. C. Stair, *Chem. Soc. Rev.*, 2010, **39**, 4820-4844; (d) E. Stavitski and B. M. Weckhuysen, *Chem. Soc. Rev.*, 2010, **39**, 4615-4625.
8. (a) E. M. van Schrojenstein Lantman, T. Deckert-Gaudig, A. J. Mank, V. Deckert and B. M. Weckhuysen, *Nature nanotechnology*, 2012, **7**, 583-586; (b) X. Tang, W. Cai, L. Yang and J. Liu, *Nanoscale*, 2014, **6**, 8612-8616; (c) V. Joseph, C. Engelbrekt, J. Zhang, U. Gernert, J. Ulstrup and J. Kneipp, *Angew. Chem. Int. Ed.* , 2012, **51**, 7592-7596; (d) W. Xie, C. Herrmann, K. Kompe, M. Haase and S. Schlucker, *J. Am. Chem. Soc.*, 2011, **133**, 19302-19305; (e) W. Xie, B. Walkenfort and S. Schlucker, *J. Am. Chem. Soc.*, 2013, **135**, 1657-1660.
9. (a) I. Yoon, T. Kang, W. Choi, J. Kim, Y. Yoo, S. W. Joo, Q. H. Park, H. Ihee and B. Kim, *J. Am. Chem. Soc.*, 2009, **131**, 758-762; (b) S. J. Lee, J. M. Baik and M. Moskovits, *Nano Lett.*, 2008, **8**, 3244-3247.
10. Q. Zhou, X. Li, Q. Fan, X. Zhang and J. Zheng, *Angewandte Chemie*, 2006, **118**, 4074-4077.
11. S. Wunder, F. Polzer, Y. Lu, Y. Mei and M. Ballauff, *Journal of Physical Chemistry C*, 2010, **114**, 8814-8820.
12. B. Dong, Y. Fang, X. Chen, H. Xu and M. Sun, *Langmuir*, 2011, **27**, 10677-10682.
13. (a) K. Kim, D. Shin, K. L. Kim and K. S. Shin, *Physical Chemistry Chemical Physics*, 2012, **14**, 4095-4100; (b) K. Kim, I. Lee and S. J. Lee, *Chemical physics letters*, 2003, **377**, 201-204; (c) S. Sun, R. L. Birke, J. R. Lombardi, K. P. Leung and A. Z. Genack, *The Journal of Physical Chemistry*, 1988, **92**, 5965-5972; (d) S. Duan, Y.-J. Ai, W. Hu and Y. Luo, *The Journal of Physical Chemistry C*, 2014, **118**, 6893-6902; (e) Y. F. Huang, H. P. Zhu, G. K. Liu, D. Y. Wu, B. Ren and Z. Q. Tian, *J. Am. Chem. Soc.*, 2010, **132**, 9244-9246; (f) L. B. Zhao, Y. F. Huang, X. M. Liu, J. R. Anema, D. Y. Wu, B. Ren and Z. Q. Tian, *Phys. Chem. Chem. Phys.*, 2012, **14**, 12919-12929; (g) Z. Zhang, T. Deckert-Gaudig and V. Deckert, *Analyst*, 2015, **140**, 4325-4335; (h) D.-Y. Wu, X.-M. Liu, Y.-F. Huang, B. Ren, X. Xu and Z.-Q. Tian, *The Journal of Physical Chemistry C*, 2009, **113**, 18212-18222.

ChemComm Accepted Manuscript

This journal is © The Royal Society of Chemistry 20xx